

Non-sticky and Free-forward Performances of Grubs against Soil

Qingwen Dai, Shaojie Qiu, Wei Huang, Xiaolei Wang*

National Key Laboratory of Science and Technology on Helicopter Transmission, Nanjing University of Aeronautics & Astronautics, Nanjing, 210016, China



ARTICLE INFO

Keywords:

Grub
Adhesion
Friction
Biological electroosmosis
Hierarchical micro structures pattern

ABSTRACT

The intriguing non-sticky and free-forward performances of grubs against soil deeply attract our interests. In this study, the life cycle and body morphology of a kind of grubs, larvae of Japanese rhinoceros beetles, are introduced. The uniformly oriented hierarchical micro structures pattern on the back epidermis is firstly reported. The rotating and forwarding motion configuration of grubs in soil is unraveled. The friction and adhesion properties of grubs are evaluated and compared with typical materials. The biological electroosmosis induced adhesion reduction effect and the hierarchical structures pattern induced anisotropic friction feature are highlighted.

1. Introduction

In agricultural machinery, a mechanical action in direct contact with soil is always accompanied by adhesion and friction processes at the surface/interface. Soil adhesion can increase the frictional resistance of vehicles on soft or wet ground [1–3]. Excessive soil adhered on soil-engaging components of earthmoving machines, such as excavator buckets or bulldozer blades, would reduce the work efficiency to about 30–50% at the expense of additional energy consumption [4]. The existing literatures reported that strategies of applying additional vibration [5], injecting gas or liquid onto the surfaces [6], heating the surfaces [7], can all reduce the soil adhesion and friction forces to some extent, while these methods are complex, expensive, and hard for practical applications. The ideal techniques should have advantages of simple structure, convenient maintenance, and no additional manipulation [8].

Bionics approach seems to be a candidate to achieve this goal. Through millions of years, soil organisms have evolved their body structures to achieve maximal performances in responding and adapting to changes in the nature [9–18]. Setae on gecko's feet contribute to a strong adhesion force for attachment and excellent self-cleaning capability [19,20]. Micro convex hollows on dung beetle's head endow a special ability to move dungs without sticking [21,22], and setae on its ventral surface and outside legs create a non-adherent interface [23]. Squama-form surface on the abdomen of ants, bristle-form surface on the backboard of mole crickets both contribute to their anti-adhesion properties [4].

It is noticed that these animals all live on soil and their bodies are in part contact with soil, earthworm is the most representative one living

in soil. It has excellent anti adhesion and friction performances when moving in soil, which are attributed to its retractable body segments and the excreted mucus for lubrication [24]. The masterpieces of nature have inspired the design of anti-adhesion surfaces of tillage machinery [25], soil robot [26] and so on [27].

Besides that, the larvae of Japanese rhinoceros beetles (Fig. 1), colloquially called grubs, also have some idiosyncratic characteristics. It lives underground and when it is excavated out, we never see soil adhered on its skin, no matter the soil is wet or dry. Fig. 1b shows three typical movement of a grub against soil and its body maintains clean. Via continuous observations, it is noticed that grubs would invariably move forward in soil via their head and front tarsi while never move backward.

These intriguing “non-sticky” and “free-forward” properties of grubs deeply attract our interests. Compared to earthworms, grubs have tarsus and do not secrete mucus when moving. Mucus can reduce the friction and adhesion forces against soil, which is the dominate feature of earthworms [28,29]. So, with a mostly dry body, how can a grub move forward freely in soil and keep the skin clean? What is the reason for these “non-sticky” and “free-forward” properties? Up to now, no reported studies focus on this aspect. Revealing the mechanism is critical for scientific research, and particularly, could provide some feasible anti adhesion and friction design strategies for soil-engaging components.

2. Grubs

Japanese rhinoceros beetles are highly popular in Asia, which are of the genus *Coleoptera*, in the family *Scarabaeidae* [30]. Naturally, their

* Corresponding author.

E-mail address: wxl@nuaa.edu.cn (X. Wang).

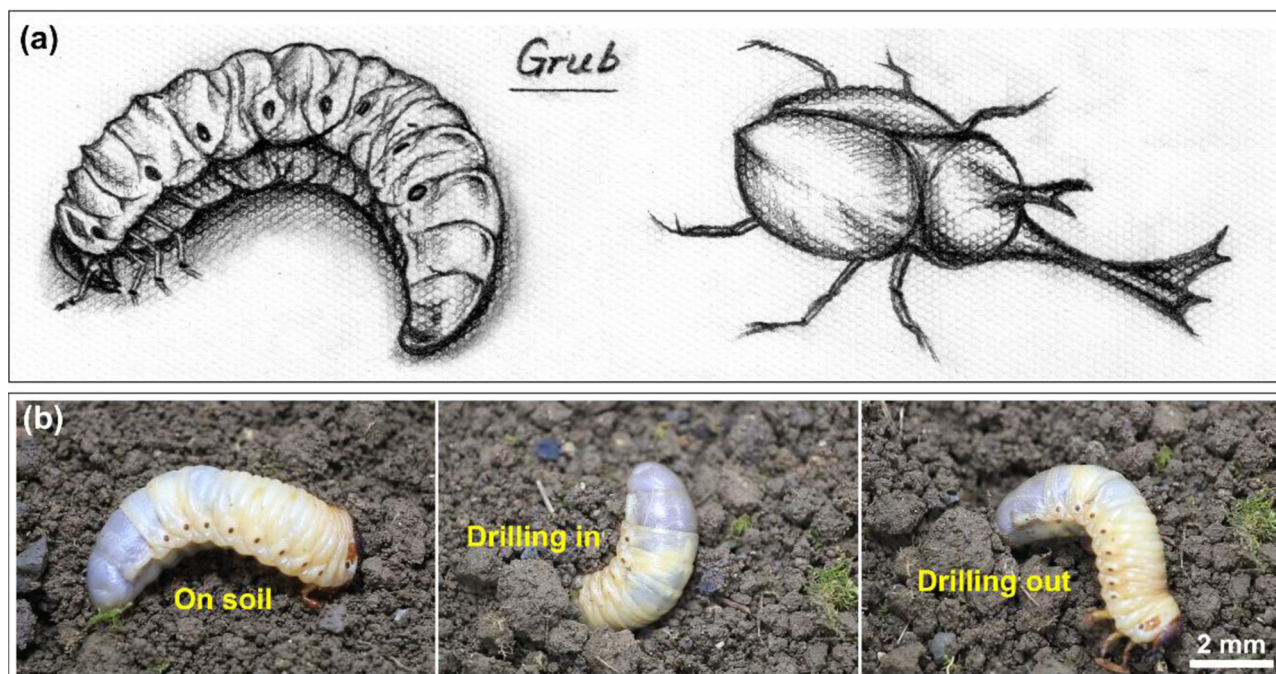


Fig. 1. (a) Sketch of a grub and Japanese rhinoceros beetle. (b) Three typical moving processes of a grub against soil.

life cycle passes through four main stages: egg, larva, nymph, and adult [31], which was observed and recorded in this work, as shown in Fig. S1. The eggs have white, smooth, and soft surface, it takes about 20 to 30 days before hatching to larva. Larva is the principal feeding stage, which lasts for about three months. It is mainly fed on plants, such as tender roots, residual seed coat, rhizomes, and etc. Then the larva pupates, and from these pupae emerge fully formed, sexually mature adult beetles. The whole metamorphosis to beetles passes through 8 months.

2.1. Morphology of grubs

In this study, the larvae of Japanese rhinoceros beetles (hereinafter referred to as grubs) are chosen for experiments, which are reared in a container filled with soil. The well-developed grubs have three pairs of front tarsi, and their length ranges from 60 to 100 mm. Fig. S2 exhibits a detailed photograph of different parts of a grub. Its head is well-developed, sclerotized, and featured with micro dimples ($\sim 300 \mu\text{m}$ in diameter). There are about ten wave-like structural segments on the body [32]. A notable feature is that pattern of micro setae structures is found on its back, and via checking the micro setae structures on each segment, it is found that all setae are oriented from the head to tail.

2.2. Motion configuration of grubs in soil

To monitor the motion of grubs in soil, a transparent PMMA chamber with appropriate dimensions of $240 \times 220 \times 30 \text{ mm}$ was prepared and fulfilled with soil. As shown in Fig. 2a, initially, the grub claws the soil in front via its head and tarsi; and the whole body moves forward in soil via successive stretching and contracting motions of segments; then it curls up and rotates until the head is downward; and then repeating the above processes. As the sketch map indicates, the motion configuration of grubs in soil is forwarding and rotating, which is a coordination action of head, tarsi and body segments. A key point during the locomotion is that the back of grub is mainly in contact with soil, which might provide a robust friction force. The whole processes can be seen in the supporting material of Video S1.

3. Experimental Sections

3.1. Sample preparation

3.1.1. Pin

In the natural world, grubs can move in soil of different moisture contents without smearing their skin. Hence, by completely drying soil, grinding it to fine powder (under 2800 mesh number), drying it again, and then changing the mass ratio of water to soil, soil specimens of different moisture contents of 25%, 27%, 29% and 33% are prepared. The moisture contents range between the liquid limit (above 35.6%, soil turns into liquid state) and plastic limit (under 21.2%, soil turns into powdery state) [33]. All specimens are kept to cylinder shapes with dimensions of 5 mm in diameter and 12 mm in height for friction and adhesion tests.

3.1.2. Disk

The epidermis on the back of grub is cut to a specified dimension of $15 \times 15 \text{ mm}$, ultrasonically cleaned in ethanol to remove impurities, and stored in a drying box for tests. It is experimentally found that the epidermis is joined together with the subcutaneous tissue, and no exact boundary exists between the epidermis and subcutaneous tissue. Its hardness and modulus of elasticity are $\sim 0.467 \text{ GPa}$ and $\sim 6.434 \text{ GPa}$, respectively (detailed measuring processes and curves are shown in Fig. S3). Three living grubs are used for tests and their body size are $\sim 80 \text{ mm}$ in length. Besides, typical materials of rubber, glass, stainless steel, and PTFE are employed for comparison. In reality, the tire and dust proof parts of ground machinery are mainly made from rubber, and the contact parts are made from stainless steel [25]. PTFE is a typical material of low friction coefficient and excellent chemical stability, and glass is widely used in ground machinery.

3.2. Adhesion and friction measurements

Fig. S4 shows the schematic diagrams of the experimental apparatuses. In order to measure the adhesion and friction forces between the soil and grub, a PMMA chamber is designed to fix the grub. The prepared epidermis is flatly attached on a glass slide via double-sided adhesive tape. All measurements are conducted at an ambient

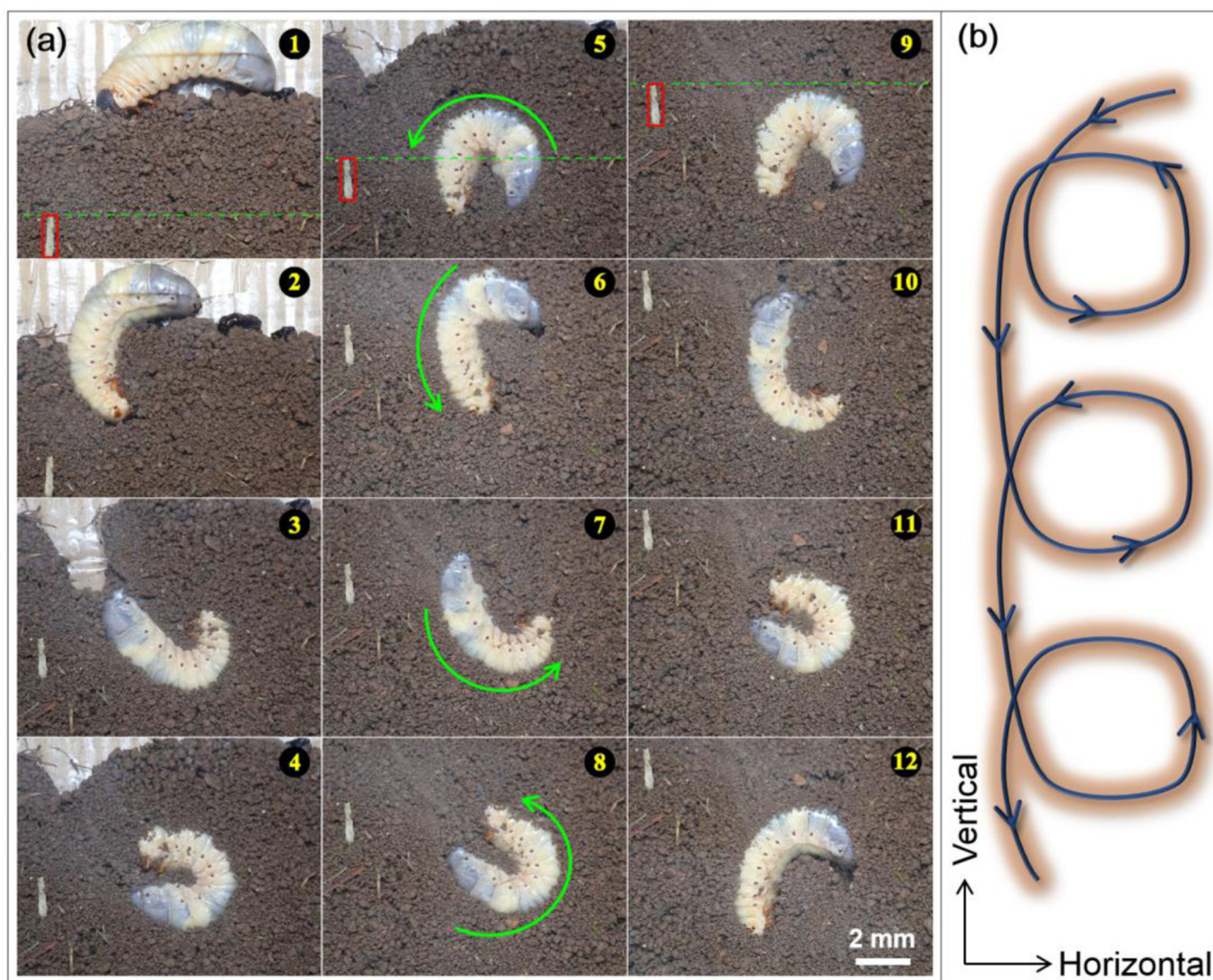


Fig. 2. (a) Motion configuration of a grub in soil; (b) Sketch map of the locomotion path.

temperature of $\sim 25^\circ\text{C}$ and humidity of $\sim 50\%$.

The adhesion testing process is as follows: driving the pin (soil) down onto the disk surface (grub, epidermis, and other materials) with a preload, holding for some time, retracting the pin until the two surfaces are detached, then the static adhesion force can be measured. Repeating the above-mentioned processes and moving the disk in the horizontal direction at the same time, the dynamic adhesion force can be measured. The adhesion force of per unit area (P) is used for comparison, which is mathematically expressed as: $P = F/A$. F and A represent the preload and contact area, respectively. After the adhesion testing, the cross-section shape of soil pins is roughly circular, and the real contact area is obtained by measuring the changed-diameter.

The friction force is measured by a pin-on-disk type friction tester, and the process is as follows: contacting the surfaces of the pin (soil) and the disk (grub, epidermis, and other materials) with a dead load, moving the disk in the horizontal direction circularly, and then the friction force can be measured. More detailed of these apparatus are available in our previous papers [34,35].

4. Results and Discussion

4.1. Soil adhesion performances

4.1.1. Static and dynamic soil adhesion performances

Fig. 3a shows the influence of soil moisture content on the static adhesion force under a preload of 2.5 N and a holding time of 50 s. A

higher soil moisture content yields a larger static adhesion force. The adhesion force on the grub is smallest, and on other surfaces, it is in ascending order of epidermis, glass, rubber, stainless steel, and PTFE. Fig. 3b presents the influence of holding time on the static adhesion force under a preload of 2.5 N and a moisture content of 29%. It can be seen that the static adhesion force on each tested surface increases smoothly with increasing holding time, and this force maintains in a lowest magnitude on the grub. An increasing preload would enhance the adhesion force significantly, when it increases from 0.5 to 4.5 N, the adhesion force increases nearly 300% on the glass surface, as shown in Fig. 3c. The overall trend of static adhesion forces on the tested surfaces is similar under different conditions, while the adhesion forces on the grub are always much lower than these on the others.

Fig. 4 presents a comparison between the static and dynamic adhesion forces of different surfaces against soil under varying soil moisture contents. The sliding speed, preload, and holding time are 15 mm/min, 2.5 N and 30 s, respectively. The epidermis is not tested due to the limited dimension for sliding. Since grubs can only move forward in soil, the dynamic adhesion force is measured within the processes from head to tail. Generally, the dynamic adhesion forces on these surfaces are much higher than the static ones. Note that the rubber has a relative low static adhesion force while a high dynamic one, which might attribute to its elasticity. Statically, the deformation of rubber under a specific load diminishes the real contact area, reducing the adhesion force; while dynamically, this deformation generates significant resistances in both tangential and normal directions,

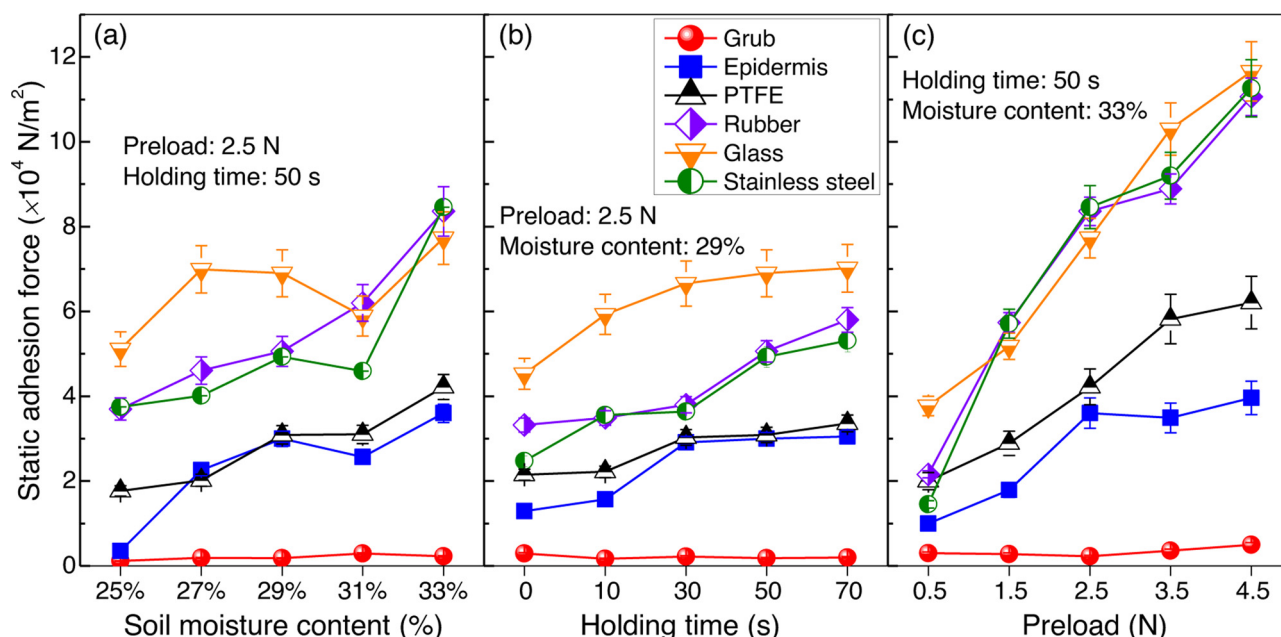


Fig. 3. Influences of (a) soil moisture content, (b) holding time, and (c) preload on the static adhesion forces between the soil and grub, epidermis, and other materials.

yielding a higher adhesion force. Note that for the grub, the static and dynamic adhesion forces maintain in a significant low magnitude, and only a slight difference exists between them. It reveals the fact in the natural world, the grub always has the “non-sticky soil” feature, no matter it moves or stays still.

4.1.2. Wetting and soil adhesion

Fig. 5a shows the apparent contact angles (θ) of deionized water on the surfaces of epidermis, grub (on the back), stainless steel, glass, rubber and PTFE, which were measured via a sessile drop method and more details of the measurement is available in [36]. It can be seen that the stainless steel, glass, and rubber are hydrophilic, while the epidermis, grub and PTFE are hydrophobic. Referring to the overall trends

of static and dynamic soil adhesion performances shown in Figs. 3 and 4, there should be a correlation between the soil adhesion performances and wetting properties.

Figs. 5b and c exhibit the enlarged sketch maps of the contact models at the interfaces of soil/hydrophilic and soil/hydrophobic surfaces, respectively. Since soil surfaces are rough and porous, water and air could easily penetrate inside soil [37]. When a soil specimen of a specific moisture content contacts a solid surface, partial soil directly contacts the solid surface, generating a soil adhesion (F_{soil}); while the others are linked to the solid surface via a water film, trapping air at the interface [38], forming a Cassie-like wetting interface. This water film could generate an irregular water loop, yielding a meniscus tension and Laplace pressure (capillary pressure) at the interface [39].

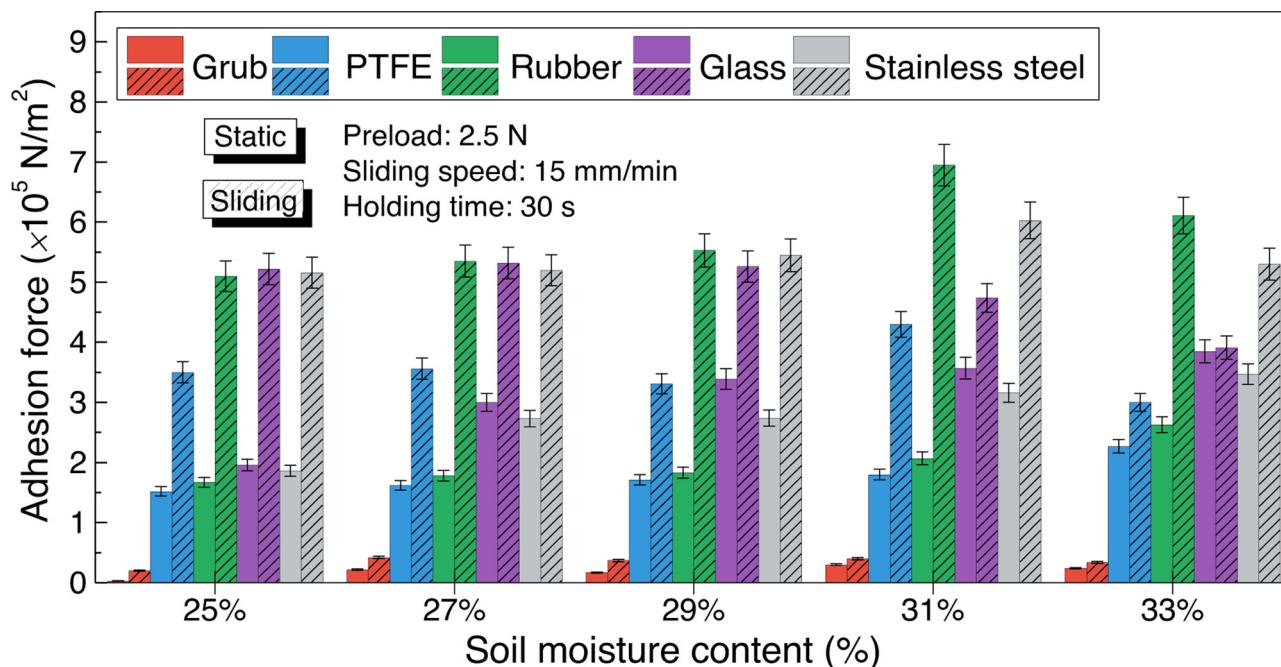


Fig. 4. Comparison between the static and dynamic adhesion forces of different surfaces against soil under varying moisture contents.

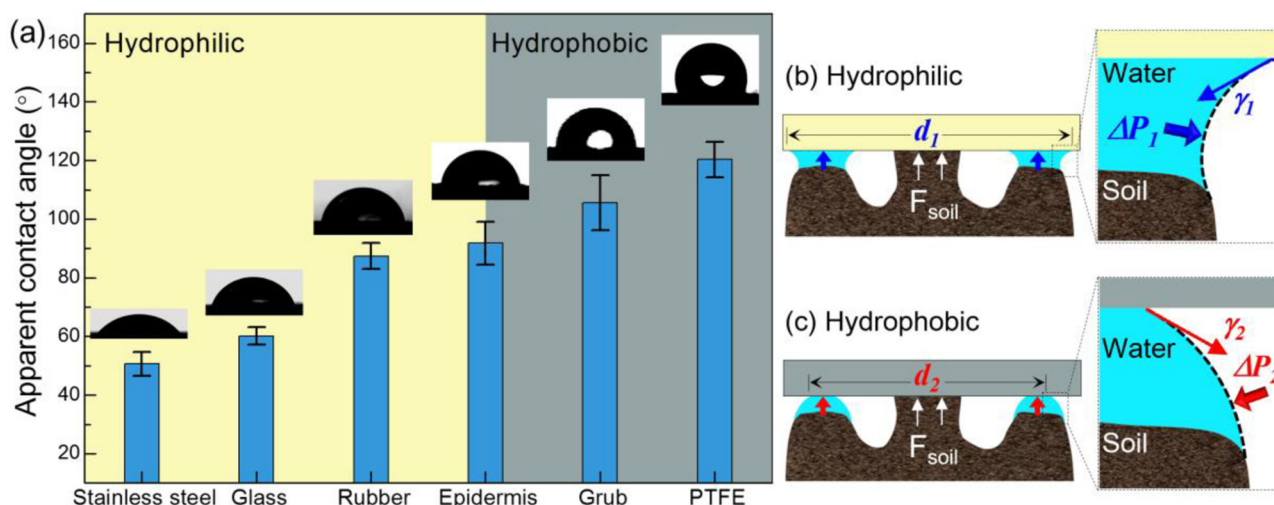


Fig. 5. (a) Apparent contact angles of deionized water on the tested surfaces. Contact models at the interfaces of: (b) soil/hydrophilic and (c) soil/hydrophobic surfaces.

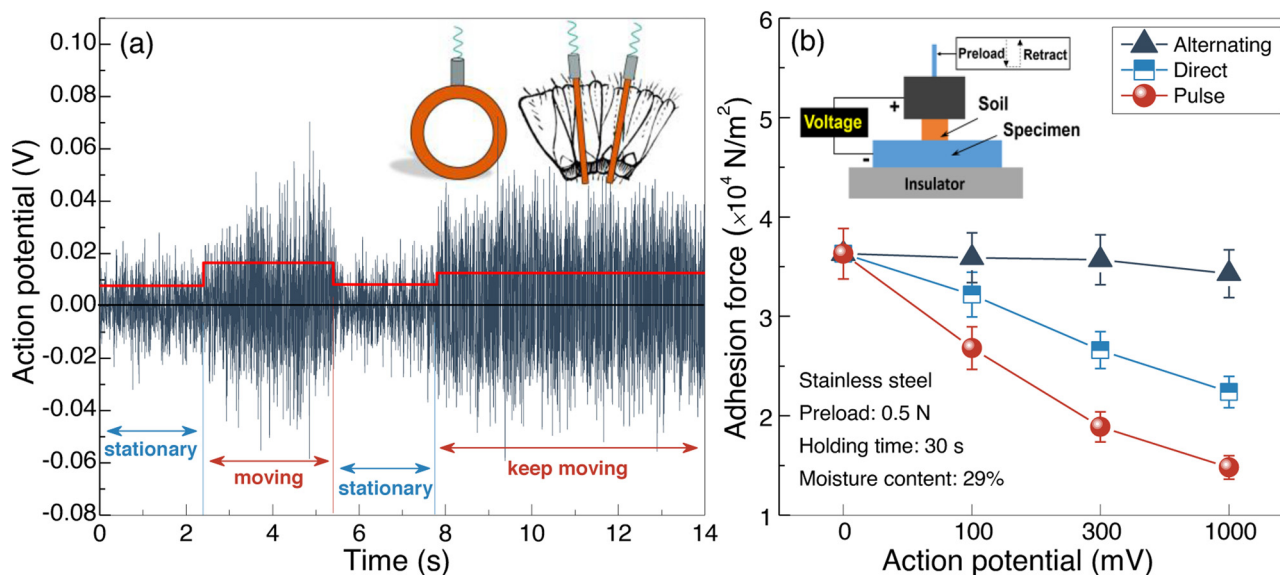


Fig. 6. (a) Measured variation in action potentials between two surface points of a living grub. (b) Influences of alternating, direct, and pulse potentials on the static adhesion force.

When the soil moisture content and contact condition are steady-state, besides the F_{soil} , the work of adhesion (W) between solid and liquid can be expressed by the Young-Dupré equation [40]:

$$W = \gamma(\cos \theta + 1) \quad (1)$$

where γ represents the surface tension of liquid. According to this formula, the apparent contact angle quantifies the work of soil adhesion, that is, the larger the contact angle is, the lower the work of adhesion will be. The experimental results basically follow this rule.

Since the wettability region of the hydrophilic surface (d_1) is larger than that of the hydrophobic one (d_2), the meniscus tension at the hydrophilic interface would make a greater contribution to the adhesion force. Moreover, it should be noticed that the capillary pressure in the loop would affect the adhesion force between the soil and solid surface within detaching processes [39]. Attributed to the different concave and convex liquid/air menisci (Fig. 5b and c), the generated capillary pressure for the hydrophilic interface (ΔP_1) is from inside (liquid) to outside (air), while from outside (air) to inside (liquid) for the hydrophobic one (ΔP_2) [41]. As a separation progresses, the adhesion force would be enhanced by ΔP_1 , while weakened by ΔP_2 on the

contrary. Moreover, most solids are rough and associated with the pinning of the contact line on surface defects, the separation process of the soil and solid surface involves the contact angle hysteresis effect [42]. As reported by Tong et al. [43], this hysteresis effect at the interface would contribute to the adhesion force.

Overall, the soil adhesion (F_{soil}) and liquid film induced meniscus tension and capillary pressure together contribute to the adhesion force. The adhesion force between the soil and hydrophobic surfaces is weaker than that of hydrophilic ones. Increasing the moisture content can contribute to this liquid capillary pressure, enhancing the adhesion force (Figs. 3a and 4). Meanwhile, a higher preload or a longer holding time makes a better contact condition between the surface and soil, strengthening the adhesion effect (F_{soil}).

Note that there is a slight difference between the wetting property of living body and epidermis, while the adhesion force on the living body is much lower than that on the epidermis under varying moisture content, holding time, or preload. These results are quite interesting, and reasons for the differences need to be further clarified.

4.1.3. Biological electroosmosis

Electroosmosis flow describe a phenomenon that water can be made to flow through a plug of clay by applying an electric voltage [44]. It has been reported that earthworms moving in soil are subjected to a local deformation by soil, generating action potentials on their surfaces [45]. For grubs, whether this phenomenon exists or not is still unknown. Therefore, we measured the variation in action potential between two surface points of a living grub (inset in Fig. 6a, and the detailed measuring process is shown in Fig. S5). Fig. 6a shows the measured action potentials and the calculated absolute values. When the grub remains stationary, the action potential is in a low amplitude of ~ 7 mV; as it moves, this potential jumps to ~ 0.16 mV. When it keeps moving, this action potential maintains in a high amplitude of ~ 0.13 mV. The results reveal the fact that action potentials do exist on the grub surface when it moves. Then, we modified the experimental setup to measure the soil adhesion force under different electric potentials, as the inset shown in Fig. 6b. Experiments are performed between the stainless steel and soil (moisture content of 29%) under a preload of 2.5 N and a holding time of 30 s. Alternating, direct, and pulse potentials are imposed between the two surfaces via a signal generator. It can be seen that the alternating potential has little effect on the adhesion force, while adhesion forces decrease to varying degrees when encountered with a direct or pulse one. Pulse potential has an excellent adhesion reduction effect, which is as high as 56.7% for a potential of 1000 mV.

The results indicate that a pulse or direct potential could ooze water from soil, forming a water-lubricated contact interface, reducing the direct contact part between soil and solid surface (F_{soil}), and then the adhesion force decreases correspondingly. Referring to Fig. 6a, the measured action potential is just between two surface points of the body, while the real locomotion of a grub in soil contains multiple parts, which could yield abundant action potentials. Moreover, the generated action potential is similar to the pulse potential. It can be inferred that these generated action potentials will yield a significant adhesion reduction effect between the grub and soil. The biological electroosmosis might be the reason for the non-sticky feature of grubs.

4.2. Soil friction performances

Fig. 7 shows the variation of friction forces of the grub and other materials against soil (moisture content of 27%) under a cycle speed of 15 mm/min and a load of 1 N. Limited by the dimension, the epidermis is not tested here. The friction force of PTFE is lowest due to its low-friction and self-lubricating abilities, and the measured results of rubber, stainless, and glass are basically consistent to the reference values of themselves [46]. It is interesting to see that for the grub, a huge difference exists between the friction forces in the forward and backward directions. Within each cycle, the backward friction force is nearly three times higher than that of the forward.

As mentioned in the *Motion configuration of grubs in soil* section, grubs mainly resort on the successive stretching and contracting of body segments to move in soil, and its back provides a robust forward friction force. Referring to the surface morphology of the back shown in Fig. S2, the micro setae are uniformly oriented from the head to tail, which should has some internal correlations with the friction behavior. Therefore, back epidermis is prepared via a standard biological sample preparation method [47], on which the micro setae structures are further conformed via the SEM. As shown in Fig. 8a, all setae incline in the same orientation, and each seta is of $\sim 40 - 50$ μm in diameter and ~ 100 μm in length. To enlarge the area on the back, it is found that the back is featured with pattern of secondary projection structures of ~ 2.5 μm in diameter. More importantly, these secondary projection structures also oriented in the same direction. In general, hierarchical micro structures pattern is conformed on the back epidermis of grubs, and all structures are uniformly oriented from the head to tail.

Fig. 8b shows the sketch map of the hierarchical micro structures

pattern on the back epidermis. Seen from this, the friction results presented in Fig. 7 is understandable. Actually, the anisotropic structures pattern on the back yields the anisotropic frictional behavior. When moving in the forward direction, these structures could reduce the real contact surface between the body and soil, yielding a lower friction force. When moving in the backward direction, these structures would not only act as barbs embedding into soil, but also furrow the soil within the movement, together increasing the friction force.

4.3. Further discussion

The non-sticky property of grubs can be determined by comprehensive impacts of the hydrophobic body surface, biological electroosmosis effect, and the unique motion configuration. Firstly, the surface of grubs is hydrophobic, the water oozing from soil could obstruct the direct contact between the soil and grubs, maintaining a clean body. Moreover, during a moving process, the biological electroosmosis effect provides enough water around the hydrophobic body, which further reduces the adhered soil on the body. Thirdly, grubs mainly resort on the successive stretching and contracting of body segments to move in soil, which generates a retrograde wave travelling along the body. The retrograde wave would strip down the adhered soil. Compared to the living body, the epidermis is dead tissue, on which the hierarchical micro structures patterns might be less upright (or less rough), based on the Cassie-Baxter wetting model [48], the apparent contact angle on the epidermis is slightly smaller than that on the living body. Besides, the epidermis no longer has biological electroosmosis effect and the unique motion configuration. These together contribute to a higher adhesion force of epidermis than the grub.

The reported investigations by Chen et al. [49,50] have revealed the fact that most biological tissues are anisotropic, which could leads to anisotropic or reversible mechanical properties. In this study, it is believed that the free-forward characteristic is attributed to the idiosyncratic motion configuration and uniformly oriented hierarchical micro structures pattern on back epidermis. Referring to Fig. 2, the forwarding movement of grub in soil is invariably accompanied with the process of body rotating. Its back keeps in contact with soil, providing the main friction force. Physically, the motion configuration can be regarded of as a retrograde wave travelling along the body. This retrograde wave activates the locomotion via the friction-induced traction. The measured soil friction forces (Fig. 7) and the uniformly oriented hierarchical micro structures pattern on back epidermis (Fig. 8) reveal the fact that as the segments stretching, the hierarchical micro structures on the back epidermis yield a significant friction force against soil, preventing the body sliding backward. When the segments contracting, these structures yield a low friction force, making the forward movement possible.

In general, when designing the soil-engaging components, imposing a pulse potential or hydrophobic treating the surfaces are feasible manners to weaken the soil adhesion behavior. While fabricating micrometer, millimeter or even macro-scale anisotropic structures on surfaces is recommended to reduce the friction force.

5. Conclusions

In the present work, to determine the mechanism of “non-sticky” soil and “free-forward” characteristics of grubs against soil, morphology and motion configuration of grubs in soil are investigated. Adhesion and friction performances of grubs are examined and compared with other materials. The relationship between the adhesion/friction properties and the morphology, mechanical and bioelectrical features of grubs are highlighted. The conclusions drawn from this study are as follows:

- 1 Grubs mainly resort on the successive stretching and contracting of body segments to move in soil. The generated retrograde wave

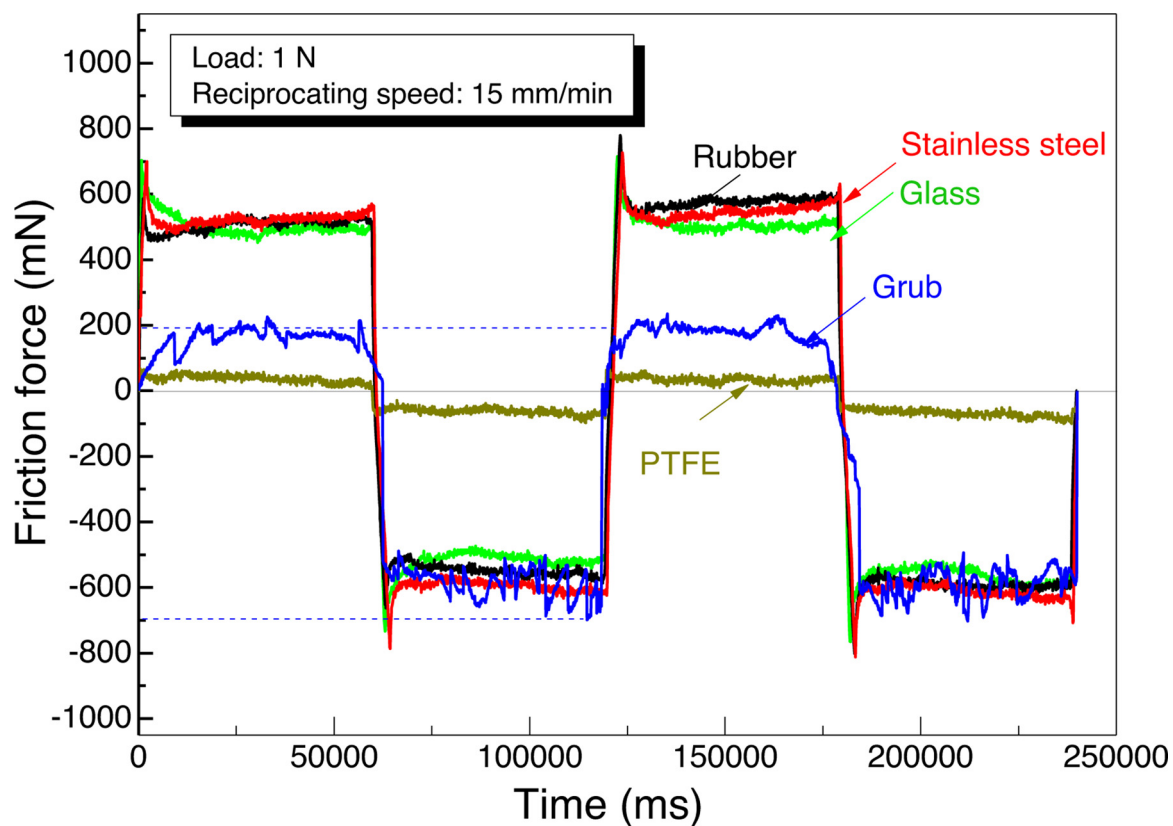


Fig. 7. Variation of friction forces of the grub and different surfaces against soil.

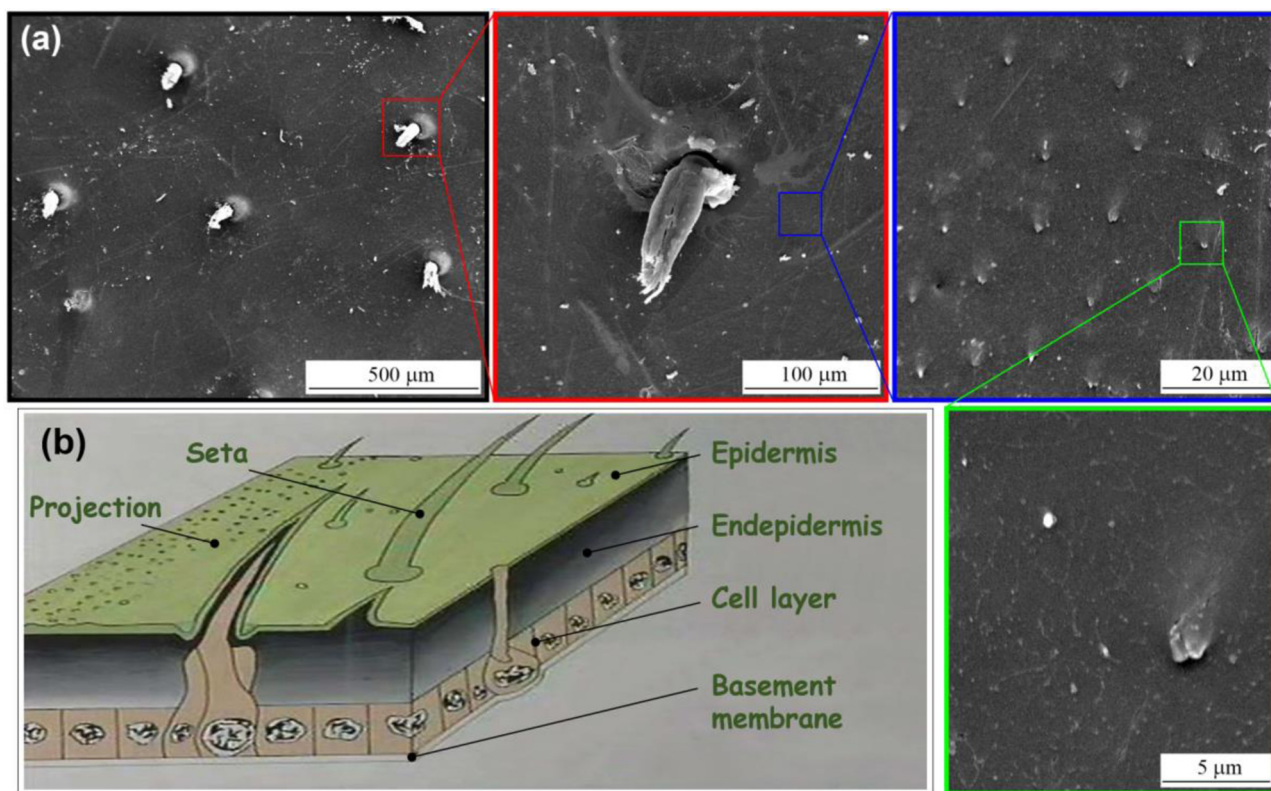


Fig. 8. (a) Progressively enlarged SEM images of the setae pattern and secondary projection structures on the back of a grub; (b) Sketch map of the hierarchical micro structures on the back epidermis.

travelling along the body activates the locomotion via the friction-induced traction. Uniformly oriented hierarchical micro structures pattern on back epidermis is firstly reported, and this anisotropic structures pattern contributes to the anisotropic frictional behavior.

- 2 The static and dynamic soil adhesion forces on the living grub's back are much lower than these on the back epidermis, as well as other typical materials of glass, rubber, stainless steel and PTFE. Increasing the moisture content of the soil, preload or longer holding time could increase the soil adhesion force. The surface of living grub's back is hydrophobic, which could yield a lower soil adhesion force than the hydrophilic ones.
- 3 Action potentials on grubs do exist when they move. Multiple action potentials could reduce the soil adhesion force effectively. Pulse potential is highly preferred to achieve an excellent soil adhesion-reduction effect.

Declaration of Competing Interest

The authors declare that they have no known competing financial interests or personal relationships that could have appeared to influence the work reported in this paper.

CRediT authorship contribution statement

Qingwen Dai: Conceptualization, Methodology, Writing - original draft. **Shaojie Qiu:** Investigation, Visualization. **Wei Huang:** Resources, Data curation. **Xiaolei Wang:** Writing - review & editing, Supervision.

Acknowledgements

The authors are grateful for the support provided by the National Natural Science Foundation of China (Grant No. 51675268). The authors would also like to thank Mr. Tao Yang, his animated painting of grubs are greatly appreciated.

References

- [1] L.Q. Ren, Z.W. Han, J.Q. Li, J. Tong, Experimental investigation of bionic rough curved soil cutting blade surface to reduce soil adhesion and friction, *Soil Till. Res.* 85 (1-2) (2006) 1–12.
- [2] L.Q. Ren, Y.H. Liang, Biological couplings: Function, characteristics and implementation mode, *Sci. China Technol. Sc.* 53 (2) (2010) 379–387.
- [3] G.J. Amador, T. Endlein, M. Sitti, Soiled adhesive pads shear clean by slipping: A robust self-cleaning mechanism in climbing beetles, *J. R. Soc. Interface* 14 (131) (2017) 20170134.
- [4] L.Q. Ren, Progress in the bionic study on anti-adhesion and resistance reduction of terrain machines, *Sci. China Ser. E: Technol. Sci.* 52 (2) (2009) 273–284.
- [5] X. Li, J. Fu, D. Zhang, T. Cui, R. Zhang, Experiment analysis on traction resistance of vibration subsoiler, *Trans. Chin. Soc. Agric. Eng.* 28 (1) (2012) 32–36.
- [6] J. Meng, X. Dong, X. Wei, Z. Yin, Fabrication of anti-adhesion surfaces on aluminum substrates of rubber plastic moulds using electrolysis plasma treatment, *AIP Adv.* 5 (4) (2015) 041304.
- [7] M.A. Khan, R. Qaisrani, J.Q. Li, The techniques of reducing adhesion and scouring soil by bionic- review of literature, *Adv. Nat. Sci.* 3 (2) (2010) 41–50.
- [8] H. Jia, W. Wang, W. Wang, J. Zheng, Q. Wang, J. Zhuang, Application of anti-adhesion structure based on earthworm motion characteristics, *Soil Till. Res.* 178 (2018) 159–166.
- [9] W.R. Hansen, K. Autumn, Evidence for self-cleaning in gecko setae, *Proc. Natl. Acad. Sci.* 102 (2) (2005) 385–389.
- [10] M. Varenberg, S. Gorb, A beetle-inspired solution for underwater adhesion, *J. R. Soc. Interface* 5 (20) (2008) 383–385.
- [11] Z. Peng, S. Chen, Effects of the relative humidity and water droplet on adhesion of a bio-inspired nano-film, *Colloids Surf., B* 88 (2) (2011) 717–721.
- [12] W.J.P. Barnes, P.J.P. Goodwyn, M. Nokhbatolfighahai, S.N. Gorb, Elastic modulus of tree frog adhesive toe pads, *J. Comp. Physiol. A* 197 (10) (2011) 969–978.
- [13] S. Hu, S. Lopez, P.H. Niewiarowski, Z. Xia, Dynamic self-cleaning in gecko setae via digital hyperextension, *J. R. Soc. Interface* 9 (76) (2012) 2781–2790.
- [14] A.G. Gillies, J. Puthoff, M.J. Cohen, K. Autumn, R.S. Fearing, Dry self-cleaning properties of hard and soft fibrillar structures, *Acs Appl. Mater. Inter.* 5 (13) (2013) 6081–6088.
- [15] S. Hu, Z. Xia, L. Dai, Advanced gecko-foot-mimetic dry adhesives based on carbon nanotubes, *Nanoscale* 5 (2) (2013) 475–486.
- [16] Z.L. Peng, C. Wang, S.H. Chen, Effects of surface wettability on gecko adhesion underwater, *Colloids Surf., B* 122 (2014) 662–668.
- [17] Q. Xu, W. Zhang, C. Dong, T.S. Sreeprasad, Z. Xia, Biomimetic self-cleaning surfaces: Synthesis, mechanism and applications, *J. R. Soc. Interface* 13 (122) (2016) 20160300.
- [18] C. Zhang, D.A. McAdams, J.C. Grunlan, Nano/micro-manufacturing of bioinspired materials: A review of methods to mimic natural structures, *Adv. Mater.* 28 (30) (2016) 6292–6321.
- [19] G. Huber, H. Mantz, R. Spolenak, K. Mecke, K. Jacobs, S.N. Gorb, E. Arzt, Evidence for capillarity contributions to gecko adhesion from single spatula nanomechanical measurements, *Proc. Natl. Acad. Sci.* 102 (45) (2005) 16293–16296.
- [20] Q. Xu, Y. Wan, T.S. Hu, T.X. Liu, D. Tao, P.H. Niewiarowski, Y. Tian, Y. Liu, L. Dai, Y. Yang, Z. Xia, Robust self-cleaning and micromanipulation capabilities of gecko spatulae and their bio-mimics, *Nat. Commun.* 6 (2015) 1–9.
- [21] A.H. Ji, L.B. Han, Z.D. Dai, Adhesive contact in animal: Morphology, mechanism and bio-inspired application, *J. Bionic Eng.* 8 (4) (2011) 345–356.
- [22] J. Sun, J. Tong, Y. Ma, Nanomechanical behaviours of cuticle of three kinds of beetle, *J. Bionic Eng. Suppl.* (2008) 152–157.
- [23] J. Sun, J. Li, H. Cheng, Z. Dai, L. Ren, Restudies on body surface of dung beetle and application of us bionics flexible technique, *J. Bionic Eng.* 1 (1) (2004) 53–60.
- [24] D. Zhang, Y. Chen, Y. Ma, L. Guo, J. Sun, J. Tong, Earthworm epidermal mucus: Rheological behavior reveals drag-reducing characteristics in soil, *Soil Till. Res.* 158 (2016) 57–66.
- [25] J. Tong, Q. Zhang, L. Guo, Y. Chang, Y. Guo, F. Zhu, D. Chen, X. Liu, Compaction performance of biomimetic press roller to soil, *J. Bionic Eng.* 12 (1) (2015) 152–159.
- [26] J. Ge, A. Calderon, N. Perez-Arancibia, An earthworm-inspired friction-controlled soft robot capable of bidirectional locomotion, *Bioinspir. Biomim.* 14 (3) (2018) 3282–3400.
- [27] J. Tong, M.A.M. Almobarak, Y. Ma, W. Ye, S. Zheng, Biomimetic anti-abrasion surfaces of a cone form component against soil, *J. Bionic Eng.* 7 (S4) (2010) S36–S42.
- [28] L.Q. Ren, Y.P. Wang, J.Q. Li, J. Tong, Flexible unsmoothed cuticles of soil animals and their characteristics of reducing adhesion and resistance, *Chin. Sci. Bull.* 43 (2) (1998) 166–169.
- [29] H. Zhao, Q. Sun, X. Deng, J. Cui, Earthworm-inspired rough polymer coatings with self-replenishing lubrication for adaptive friction-reduction and antifouling surfaces, *Adv. Mater.* 30 (29) (2018) 1802141.
- [30] P. Bouchard, Y. Bousquet, A.E. Davies, M.A. Alonso-Zarazaga, J.F. Lawrence, C.H.C. Lyal, A.F. Newton, C.A.M. Reid, M. Schmitt, S.A. Slipiński, A.B.T. Smith, Family-group names in coleoptera (insecta), *ZooKeys* 88 (2011) 1–972.
- [31] S.D. Beck, R.K. Bharadwaj, Reversed development and cellular aging in an insect, *Science* 178 (4066) (1972) 1210–1211.
- [32] C. Gillott, *Entomology*, Springer-Verlag, 1995.
- [33] B. Sharma, P.K. Bora, Plastic limit, liquid limit and undrained shear strength of soil-reappraisal, *J. Geotech Geoenviron* 129 (8) (2003) 774–777.
- [34] Z. Wang, Z. Hu, W. Huang, X. Wang, Elastic support of magnetic fluids bearing, *J. Phys. D: Appl. Phys.* 50 (43) (2017) 435004.
- [35] W. Huang, X. Wang, Biomimetic design of elastomer surface pattern for friction control under wet conditions, *Bioinspir. Biomim.* 8 (4) (2013) 46001–46006.
- [36] W. Dai, W. Huang, X.L. Wang, Contact angle hysteresis effect on the thermo-capillary migration of liquid droplets, *J. Colloid Interface Sci.* 515 (2018) 32–38.
- [37] S.K. Woche, M.-O. Goebel, M.B. Kirkham, R. Horton, R.R.V. Ploeg, J. Bachmann, Contact angle of soils as affected by depth, texture, and land management, *Eur. J. Soil Sci.* 56 (2005) 239–251.
- [38] J. Tong, L.Q. Ren, B.C. Chen, A.R. Qaisrani, Characteristics of adhesion between soil and solid surfaces, *J. Terramechanics* 31 (2) (1994) 93–105.
- [39] E.R. Fountaine, Investigations into the mechanism of soil adhesion, *J. Soil Sci.* 5 (2) (1954) 251–263.
- [40] B. E, *Wetting of real surfaces*, de Gruyter, Berlin, 2019.
- [41] P.-G.D. Gennes, F. Brochard-Wyart, D. Quéré, *Capillarity and wetting phenomena*, Springer, Berlin, 2003.
- [42] H.Y. Erbil, *Surface chemistry of solid and liquid interfaces*, Blackwell, Oxford, 2006.
- [43] L.Q. Ren, J. Tong, J.Q. Li, B.C. Chen, Soil adhesion and biomimetics of soil-engaging components: A review, *J. Agric. Eng. Res.* 79 (3) (2001) 239–263.
- [44] N.A. Patankar, H.H. Hu, Numerical simulation of electroosmotic flow, *Anal. Chem.* 70 (9) (1998) 1870–1881.
- [45] B. Li, Y.Y. Yan, Solid desiccant dehumidification techniques inspired from natural electroosmosis phenomena, *J. Bionic Eng.* 8 (1) (2011) 90–97.
- [46] S.Z. Wen, P. Huang, *Principles of tribology*, Tsinghua University Press, Beijing, 2008.
- [47] S. Wang, M. Li, W. Huang, X. Wang, Sticking/climbing ability and morphology studies of the toe pads of chinese fire belly newt, *J. Bionic Eng.* 13 (1) (2016) 115–123.
- [48] D. Quéré, Wetting and roughness, *Annu. Rev. Mater. Res.* 38 (1) (2008) 71–99.
- [49] S. Chen, H. Gao, Bio-inspired mechanics of reversible adhesion: Orientation-dependent adhesion strength for non-slipping adhesive contact with transversely isotropic elastic materials, *J. Mech. Phys. Solids* 55 (5) (2007) 1001–1015.
- [50] Z. Peng, C. Wang, Y. Yang, S. Chen, Effect of relative humidity on the peeling behavior of a thin film on a rigid substrate, *Phys. Rev. E* 94 (3-1) (2016) 032801.